Journal of Colloid and Interface Science 702 (2026) 139008

Contents lists available at ScienceDirect

Journal of Colloid And Interface Science

journal homepage: www.elsevier.com/locate/jcis

Characterization of lipid solubilization, bicelle formation, and magnetic-alignment induced by saponins

Samuel D. McCalpin [a,b,c], Kailey Kassinger [a,b], Madison Gilmore [a,b], Ayyalusamy Ramamoorthy [a,b,c,*]

[a] Department of Chemical and Biomedical Engineering, FAMU-FSU College of Engineering, Tallahassee, FL 32310, USA
[b] National High Magnetic Field Laboratory, Florida State University, Tallahassee, FL 32310, USA
[c] Institute of Molecular Biophysics, Florida State University, Tallahassee, FL 32304, USA

HIGHLIGHTS

- Crude Quillaja saponins solubilized phospholipids and formed bicelles.
- Bicelle formation depended on temperature, saponin-lipid ratio, and ionic strength.
- Triterpenoid saponins aescin, GA, Grb1, and HC dissolved lipids and formed bicelles.
- The steroid saponin digitonin dissolved lipids but did not form bicelles.

GRAPHICAL ABSTRACT

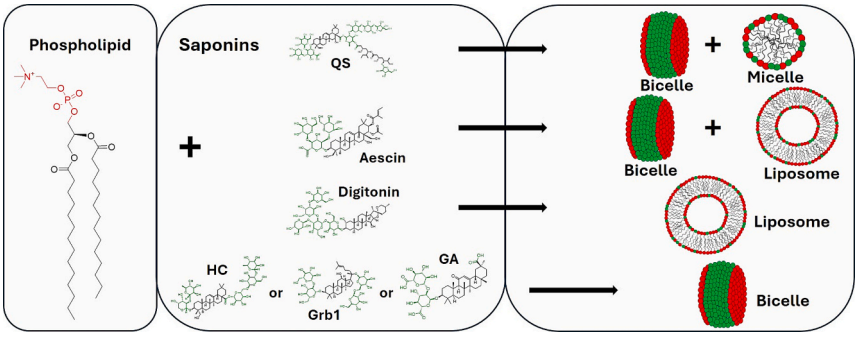

ARTICLE INFO

Keywords:
Lipid
Saponin
Bicelle
Nanodisc
Magnetic alignment
NMR

ABSTRACT

Saponins are a diverse class of plant-derived glycoside natural products. They are amphiphilic surfactants and have been included in food, agriculture, cosmetics, cleaner, and pharmaceutical products as emulsifiers. Interactions between saponins and lipids have been widely studied for these applications. Recently, some binary saponin-phospholipid mixtures have been reported to form disc-shaped colloidal particles, called bicelles or nanodiscs, that align in a magnetic field. These bicelles are potentially useful for a variety of research and biomedical purposes. Here, we used transmittance assays to determine the ability of *Quillaja* saponins (CQS) to solubilize phospholipids with varied chain lengths and headgroup charges. Then, we used static ^{31}P solid-state NMR to construct a temperature-composition diagram of the binary CQS-DMPC system and identify the conditions that allow formation of bicelles and spontaneous alignment in a magnetic field. To improve the homogeneity and reproducibility of bicelle formulations, we investigated lipid solubilization and bicelle formation of DMPC in the presence of seven additional saponin molecules and mixtures. We discovered that the triterpenoid saponins aescin, glycyrrhizic acid, ginsenoside Rb1, and hederacoside C efficiently solubilized DMPC and induced the formation of homogeneous bicelles. The steroid saponin digitonin dissolved DMPC but did not form bicelles. Possible structural determinants of saponin-induced lipid solubilization and bicelle formation are discussed.

* Corresponding author at: Department of Chemical and Biomedical Engineering, FAMU-FSU College of Engineering, Tallahassee, FL 32310, USA.
E-mail address: aramamoorthy@fsu.edu (A. Ramamoorthy).

https://doi.org/10.1016/j.jcis.2025.139008
Received 8 May 2025; Received in revised form 5 September 2025; Accepted 11 September 2025
Available online 12 September 2025

1. Introduction

Saponins comprise a diverse class of glycoside natural products with applications in food and beverages, pharmaceuticals, cosmetics, cleaners, and oil recovery [1–12]. They are amphiphilic molecules, consisting of a fused ring aglycone – called sapogenin – and one or more carbohydrate chains [10]. The sapogenin structure can contain a triterpene or steroid backbone, and saponins are broadly categorized as either triterpenoid or steroid. Almost all saponins attach a carbohydrate chain at the sapogenin C3 [10,13,14]. Bidesmosidic saponins have an additional carbohydrate chain, typically at C28 in triterpenoids or C26 in steroids [10]. These carbohydrate chains can contain between two and five monosaccharide units in a linear or branched sequence [10]. Having clearly defined hydrophobic (sapogenin) and hydrophilic (carbohydrate) regions, most saponins behave as surfactants, and most applications leverage their surfactant properties [6]. For example, saponins are commonly used as emulsifiers in food and beverages, lotions, soaps, detergent cleaners, and oil recovery processes [2].

As surfactants, saponins have also been widely demonstrated to interact with and dissolve lipid membranes [15–23]. In humans, saponins often interact with immune cell receptors and membranes, resulting in immunomodulatory effects [24–32]. Extensive research has demonstrated anti-inflammatory effects of select saponin molecules and explored their use in treating conditions such as inflammatory bowel disease [33–36]. Saponins are also commonly used for their immunostimulatory effects as adjuvants in veterinary vaccines [9,37–39]. Recently, saponins extracted from *Quillaja saponaria* have similarly been included in vaccines for shingles and COVID-19 and approved for human use [9,40,41]. However, the ability of many saponins to dissolve cell membranes also often causes hemolysis or other cytotoxic effects in high doses, limiting their biological uses except as antimicrobials or pesticides [42]. Hemolytic activity and cytotoxicity of saponins are structure-dependent, so discovering or synthesizing saponins with low toxicity is an active research goal [19,43–45].

While saponins have been extensively studied for their partitioning into lipid monolayers and spherical model lipid bilayers, a few have been additionally shown to remodel phospholipid nanoparticles to planar membrane structures [46–54]. Within certain ranges of temperatures and compositions, saponins and phospholipids self-assemble in water with the lipids forming a flat bilayer and the saponin localized around the rim, like a belt, to protect the hydrophobic lipid chains from the solvent. Hellweg et al. observed sheets and disc-shaped particles, sometimes called nanodiscs, formed by binary mixtures of the saponins β-aescin or glycyrrhizic acid (GA) with the zwitterionic phospholipid DMPC [46,50]. Similarly, our group previously reported the formation of discoidal particles by mixtures of DMPC and a crude *Quillaja* saponin (CQS) extract [54]. Traditionally, planar lipid bilayers such as these were called bicelles and considered to only adopt a discoidal geometry. However, subsequent research demonstrated that they can also assume cylindrical, ribbon, or elongated sheet morphologies, as observed for the mixtures of β-aescin and DMPC [55–58]. In this report, we will collectively refer to all non-spherical mixed bilayer micelles, including discs, cylinders, ribbons, and sheets, as bicelles.

Bicelles, especially nanodiscs, are of academic and medical interest due to their geometric, optical, and magnetic properties. Flat membranes are better models of the lipid environment around proteins in large cell membranes than curved liposome membranes and are thus attractive model membrane systems for constituting membrane proteins. In the presence of an applied magnetic field, bicelles spontaneously align with their bilayer normals oriented perpendicular to the magnetic field axis [59,60]. Aligned bicelles can serve as an anisotropic medium for NMR-based structural studies of molecules embedded within a lipid bilayer or in the solution phase [61,62]. Some research further suggests that nanodiscs have favorable geometric properties for biodistribution compared to liposomes, which makes them a promising vehicle for drug delivery [63–68].

Lipids included in bicelles are generally restricted to those that are similar to biological lipids, so there is more opportunity to vary bicelle properties via the belt. Classes of molecules commonly used as bicelle belts are detergents, short-chain phospholipids, membrane scaffold proteins, and synthetic polymers [59,69–71]. Lipid transition temperatures, lipid mobilities, compatibility of lipids, bicelle diameter and width, charge, stability against pH and metal ions, resistance to aggregation and hydrolytic degradation, membrane hydration, and temperature and composition ranges allowing magnetic alignment all depend at least somewhat on the belt [59,69,72–75]. Electrostatic properties of the belt are especially notable as many are highly charged, which may cause unwanted electrostatic interactions with molecules partitioned in the lipid bilayer or in solution. For example, our lab showed that the charge of the belt can affect the ability of nanodiscs to reconstitute membrane proteins [76]. Strong charges in the belt may also limit the ability of the bicelle to incorporate lipids of the same charge. Additionally, detergent and short-chain phospholipid belt molecules are prone to mixing within the lipid bilayer and forming micelles in solution, which might alter how the bicelle sample interacts with other molecules or proteins [54,73,77]. Thus, there is a need to identify and develop bicelle systems with belts exhibiting a range of properties. Because saponins are so structurally diverse, they are an attractive class of molecules to study for bicelle formulations.

Saponin-based bicelles are capable of both reconstituting membrane proteins and retaining motionally-averaged anisotropic interactions to enable high resolution structural studies using solution and solid-state NMR experiments [52,54]. Bicelles formed from β-aescin and DMPC were shown to accommodate bacteriorhodopsin [52], and aligned CQS-based bicelles allowed measurement of residual dipolar couplings (RDCs) for aqueous cytochrome C [54]. However, the RDCs measured using aligned CQS bicelles were weak, and β-aescin is an acidic molecule, potentially introducing unwanted electrostatic interactions with proteins embedded in the bicelle lipid bilayer and limiting the use of anionic lipids. Given the diversity of saponin structures, saponin molecules may exist that are nonionic and create a strong, homogeneous aligned phase with a variety of lipids. As such, there is a benefit to thoroughly studying the formation of bicelles with saponins. Here, we used ^{31}P solid-state NMR to study the nanoparticle structures of mixtures of DMPC and CQS. We analyzed this data to construct a temperature-composition diagram of the binary surfactant system and to identify factors that promote the formation of planar lipid bilayers that align in a magnetic field. Then, we characterized the lipid solubilization and aligned phase formation by other saponins, and identified structural features of saponins that may affect both phenomena.

2. Experimental methods

2.1. Materials

The phospholipids 1,2-dimyristoyl-sn-glycero-3-phosphocholine (DMPC, >99 %), 1,2-dipalmitoyl-sn-glycero-3-phosphocholine (DPPC, >99 %), 1,2-distearoyl-sn-glycero-3-phosphocholine (DSPC, >99 %), and 1,2-dimyristoyl-sn-glycero-3-phospho-(1′-rac-glycerol) (DMPG, >99 %) were purchased from Avanti Research (Alabaster, AL). Ginsenoside Rb1 (>97.5 %) and glycyrrhizic acid monoammonium salt (>98 %) were obtained from Thermo Fisher (Waltham, MA). Aescin (>95 % saponin content) was provided by Cayman Chemicals (Ann Arbor, MI), and all other chemicals, including the *Quillaja* saponins, digitonin (>94 %), hederacoside C (>95 %), and α-hederin (>95 %), came from Millipore Sigma (Burlington, MA). Crude (<70 % saponin content) and purified (>99.5 % saponin content) *Quillaja* saponins were purchased separately. All chemicals were used without further purification.

2.2. Lipid solubilization assay

Phospholipid stocks were prepared by weighing out the lipid and

dispersing in sodium phosphate buffer (10 mM $NaPO_4$, 100 mM NaCl, pH 7.4) for a concentration of 10 or 20 mg/mL. Before mixing with the saponins, phospholipid suspensions were subjected to 3 freeze/thaw cycles in liquid N_2 and warm water. Stocks of water-soluble saponins were made in buffer at 200 mg/mL (*Quillaja* saponins, aescin) or their solubility limit (100 mg/mL for digitonin, 40 mg/mL for Grb1). Saponin and phospholipid stocks were then added together and mixed for at least 30 min at a temperature that was at least 5 K above the phase transition temperature of the phospholipid. For samples with water-insoluble saponins (i.e. glycyrrhizic acid, hederacoside C, α-hederin), 4× saponin was dissolved directly in 10 mg/mL phospholipid, diluted with phospholipid solution without saponin for different ratios, and mixed as described previously. After mixing, 30 μL of each sample was added in triplicate to a 384-well, black-walled microplate. Absorbance was read at 790 nm using a Biotek Synergy 2 microplate reader with the incubator set to 298 K. Each sample was measured twice, and replicates were averaged. Absorbance of buffer alone was subtracted from the sample absorbance values, and transmittance was calculated for each sample as the negative log of the absorbance. Transmittance values were normalized and plotted against the mass percentage of saponin in each sample. The saponin content is reported as the mass of saponin divided by the total surfactant mass (lipid + saponin):

$$\chi_{sap} = \frac{m_{sap}}{m_{sap} + m_{lipid}}$$

Normalized transmittance data were fitted with a Boltzmann sigmoid.

2.3. NMR

Saponin/phospholipid mixtures were prepared for NMR as described above except with 100 mg/mL total phospholipid concentration and using tris buffer (10 mM tris, 100 mM NaCl, pH 7.4) instead of sodium phosphate. When saponin solubility allowed, 2× saponin and phospholipid stocks were mixed. Otherwise, saponin was dissolved directly in a 100 mg/mL phospholipid solution that had been subjected to three freeze/thaw cycles. After the saponin was added to or dissolved in the phospholipid solution, three more freeze/thaw cycles were applied to the mixture. The mixture was then packed in a thin-walled 2.5 mm Bruker rotor (approximately 25 μL volume). A typical sample contained approximately 2.5 mg of DMPC. ^{31}P NMR data were collected from 295 K – 320 K using a 400 MHz Bruker spectrometer equipped with a 2.5 mm triple-resonance HXY Bruker MAS probe operating under static conditions. Samples equilibrated at each temperature for 34 min prior to data collection by direct acquisition with ^{1}H decoupling. Acquisition parameters were 2.2 μs 90° pulse, 3 s recycle delay, and 1024 scans signal averaging. The ^{31}P chemical shift was calibrated with phosphoric acid set to 0 ppm. Data were processed with 20 Hz exponential line broadening.

3. Results and discussion

3.1. CQS dissolves phospholipids

Phospholipids suspended in aqueous buffer appear as an opaque, milky white solution. Addition of an additional surfactant can cause the solution to become transparent as the second surfactant dissolves the large, light-scattering liposomes into smaller, optically transparent species, such as micelles or nanodiscs. The dissolution of phospholipids during titration of an additional surfactant can therefore be evaluated quantitatively by measuring the transmittance of light through the sample, calculated from the absorbance of a wavelength that is not absorbed by any molecule in the sample. We measured the ability of CQS to solubilize phospholipids with varied alkyl chain length and charge via this method (Fig. 1b,c). The CQS effectively solubilized the zwitterionic phospholipids with a sigmoidal relationship between transmittance and CQS content (Fig. 1b). The amount of CQS required to dissolve the zwitterionic lipids correlated positively with the lipid alkyl chain length. The solubilization assays were performed at 298 K, which is above the main phase transition temperature (T_m) for DMPC but below the T_m of DPPC and DSPC. However, increasing the temperature during the assay did not significantly alter the solubilization profiles (**Fig. S2**), so the lipid phase cannot fully explain the differences between the solubilization behaviors of the different lipids.

In contrast, the anionic lipids exhibited a much different solubilization profile to the zwitterionic lipids (Fig. 1c). For pure DMPG, transmittance increased linearly with CQS content from 1 %–29 % CQS by weight before reaching a plateau. The plateau held through 29 %–48 % CQS, after which adding more saponin caused the transmittance to decrease, reaching 0 with 80 % CQS. A 1:1 mixture of DMPC and DMPG exhibited a solubilization behavior that combined aspects of the solubilization of the individual lipids. Transmittance increased sigmoidally with titration of low amounts of CQS before adding more CQS caused the transmittance to decrease. As with the zwitterionic lipids, the sigmoidal phase of increasing transmittance likely corresponded to a dissolution of DMPG vesicles to smaller aggregates, such as micelles, bicelles, or small vesicles. The behavior at high CQS concentration is more peculiar but has some precedent. In the presence of Ca^{2+}, moderate amounts of a polyelectrolyte dextran sulfate added to PC vesicles increased the turbidity of the solution [78,79]. This was explained as dextran sulfate adsorbed to the vesicle surface promoting vesicle aggregation via a bridging mechanism [78,79]. It is possible that CQS similarly promotes fusion of DMPG aggregates by adsorbing to the lipid particle surface and screening the surface charge. Alternatively, CQS is known to form turbid aggregates at high concentrations, so the CQS itself may be forming an aggregate with an affinity for DMPG [80,81]. The small decrease in the transmittance of samples with DMPC at high CQS concentrations may arise from a similar phenomenon (Fig. 1b,c).

3.2. Mixtures of CQS and DMPC form an impure aligned phase within a defined temperature-composition range

Transmittance provides a general picture of the solubilization of large, insoluble liposomes to small, soluble aggregates but cannot discriminate between surfactant particles with similar light scattering properties. Crucially, it cannot distinguish planar structures that align in a magnetic field from spherical particles if they are similarly soluble or insoluble, such as stacked sheets from liposomes or small bicelles from micelles. To more fully understand the self-assembly of CQS/DMPC nanoparticles and to identify the sample conditions that create a magnetically aligning phase, we acquired ^{31}P NMR spectra of CQS-DMPC mixtures with different mass ratios in the temperature range 295 K – 320 K (Fig. 2, **S3**). DMPC alone formed liposomes and gave rise to an axially symmetric powder pattern in the ^{31}P NMR spectra (Fig. 2a). The DMPC powder pattern exhibited a perpendicular edge near −17 ppm with a small temperature dependence. Increasing the temperature caused the perpendicular edge to shift to higher frequency, reflecting increased mobility of the lipids in the bilayer and decreased hydrogen bonding with the bulk water. The low intensity parallel edge appeared near 30 ppm and shifted slightly (< 1 ppm) to lower frequency at 320 K.

When we titrated CQS into the lipids, we observed three categories of NMR lineshapes depending on the mass fraction of the saponin (Fig. 2). With low CQS content (<33.3 %), the dominant ^{31}P lineshape component was still a powder pattern with a clear parallel edge above the noise level (Fig. 2b). However, the perpendicular edge was shifted downfield at low temperatures, near −14.5 ppm. As the temperature increased, the chemical shift of the perpendicular edge decreased to −17 ppm, the chemical shift observed for DMPC alone. Within this composition range, increasing CQS content also decreased the spectral intensity. Above 33.3 % CQS, the powder pattern was replaced by a symmetric peak at the perpendicular edge with no parallel edge of a powder pattern visible above the noise level (Fig. 2c). The temperature dependence of this peak

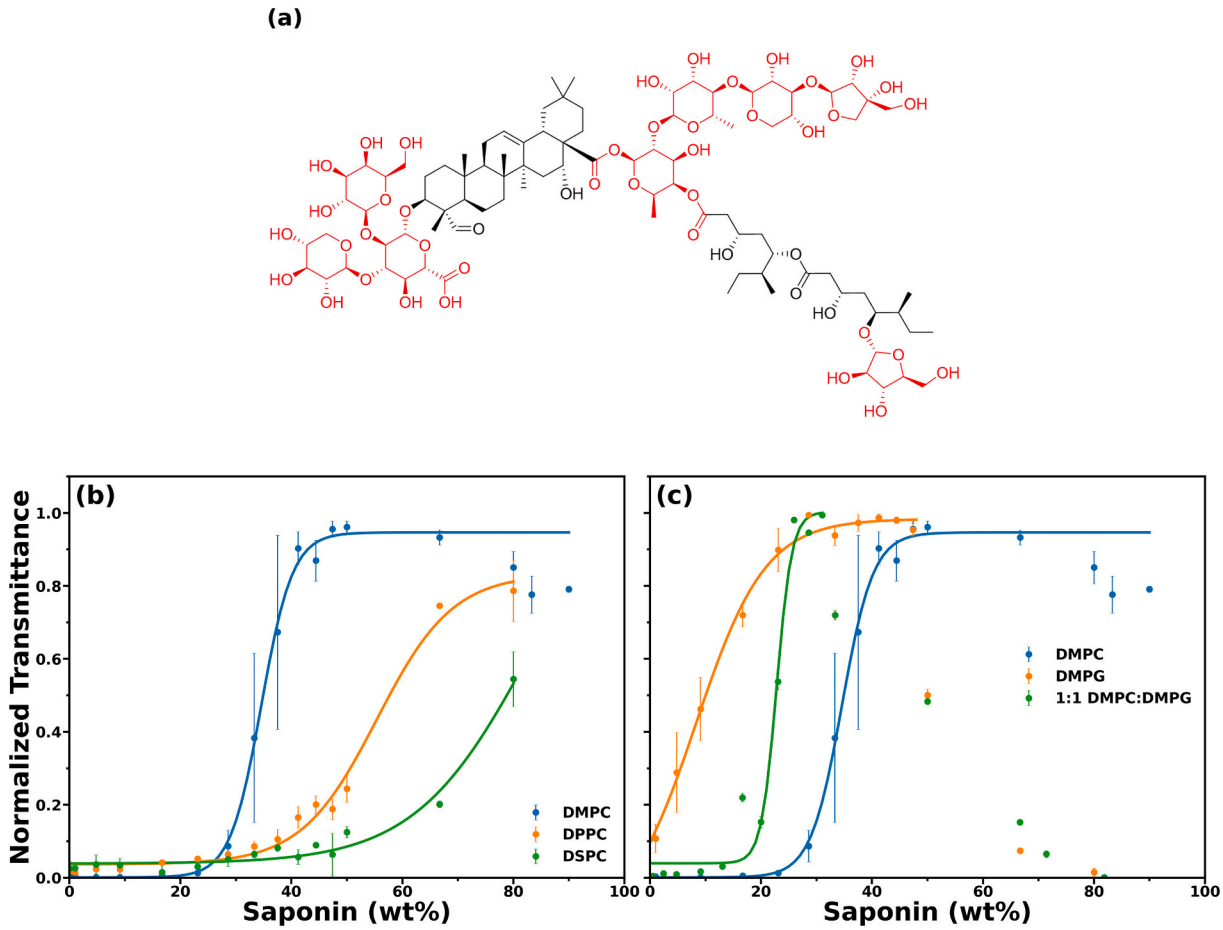

Fig. 1. Solubilization of phospholipids by CQS. (a) Chemical structure of QS-21, a major component of *Quillaja* saponins. Hydrophobic portions are in black, hydrophilic in red. Phospholipids with different (b) chain lengths (14, 16, or 18 carbons) or (c) charge were mixed with CQS in varied mass ratios. Phospholipid concentration was held constant at 10 mg/mL in each sample. The saponin mass fraction is given relative to total surfactant concentration. Samples were mixed at 5 K above gel to liquid crystalline phase transition temperature of the lipid (T_m) and then equilibrated at 298 K or 310 K. Absorbance was measured at 790 nm and converted to transmittance. A Boltzmann sigmoid was fitted to the transmittance data. The full fit parameters are provided in Table S1. Transmittance data plotted as a function of the mass ratio between the lipid and the saponin are provided in Fig. S1. (For interpretation of the references to colour in this figure legend, the reader is referred to the web version of this article.)

was similar to that of the low-CQS samples, and its intensity was greatest for the samples with CQS content around 43 %. Additional CQS caused the peak intensity to decrease to zero at 67 % CQS (Fig. 2d). Mixtures with greater than this amount of CQS gave a single peak in the ^{31}P NMR spectrum at the isotropic frequency, approximately −1 ppm. A similar isotropic peak was observed for every sample with CQS, but it only became the dominant peak at high CQS mass fractions (Fig. 2d).

The powder pattern, symmetric peak near −14 ppm, and isotropic peak at −1 ppm are attributed to a non-orienting lamellar phase, an oriented planar lamellar phase, and an isotropic phase, respectively. In the context of surfactant particle structures, the non-orienting lamellar phase generally corresponds to liposomes, the orienting phase to stacked sheets or disk-shaped bicelles, and the isotropic phase to small vesicles or micelles. Thus, the sample regimes represented by the spectra in Fig. 2 represent (i) pure liposomes (Fig. 2a), (ii) liposomes coexisting with isotropic species (Fig. 2b), (iii) orienting bicelles coexisting with isotropic species (Fig. 2c), and (iv) pure isotropic species (Fig. 2d). By analyzing the ^{31}P spectral line shapes in this way, we have constructed a temperature-composition diagram to indicate the temperatures and compositions that form each phase (Fig. 3). The shape of the region of the temperature-composition diagram corresponding to the aligned phase is similar to that of the bicelle forming region previously reported for DHPC/DMPC mixtures, with higher mass fractions of CQS pushing the temperature range for magnetic alignment higher [82]. However, the composition range that allows alignment is slightly different than what we reported previously [54]. Previously, we found that the optimal CQS mass fraction for alignment was 33.3 % and that alignment did not occur with 50 % or more CQS. However, here we show that our mixture did not align with 33.3 % CQS and that strong alignment occurred with 50 % CQS. An isotropic phase was also observed at every CQS content here, while we did not previously observe an isotropic phase for the 33.3 % CQS sample except at high temperature. The buffer composition in our prior study was slightly different to that used here, with 40 mM NaCl instead of 100 mM, so we first hypothesized that ionic strength may have contributed to these differences. It has been shown that ionic strength can alter the temperatures and compositions that allow magnetic alignment of DHPC/DMPC bicelles [82].

To test this hypothesis, we performed lipid solubilization assays and acquired temperature-dependent ^{31}P NMR spectra of CQS/DMPC mixtures with different NaCl concentrations (Fig. 4). CQS efficiently dissolved DMPC at all ionic strengths between 0 and 1 M NaCl. The amount of CQS required to solubilize the lipids did not appreciably change based on the ionic strength. However, there was a strong relationship between the slope of the transmittance curve and the ionic strength. With low ionic strength, the solubilization relative to CQS content was gradual compared to that with higher ionic strength (Fig. 4a, blue curve versus orange curve). In other words, the range of CQS contents causing partial solubilization of DMPC was greater with low ionic strength but centered

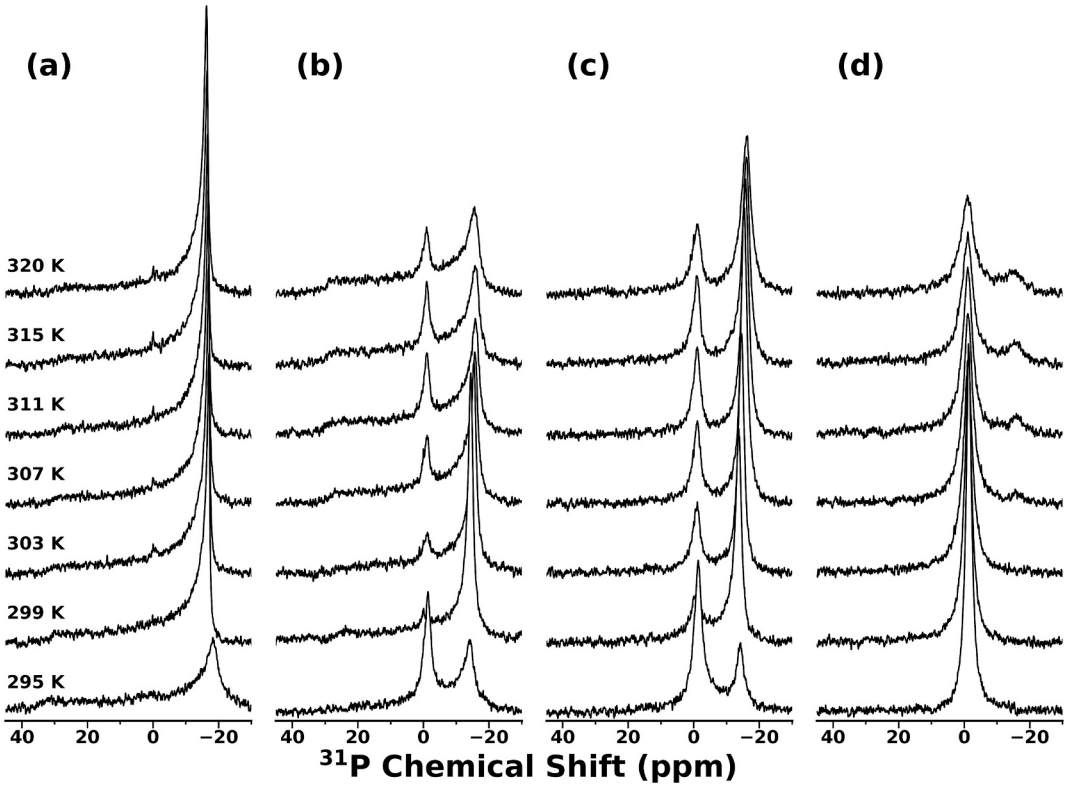

Fig. 2. Temperature-dependent phase behavior of mixtures of DMPC and CQS. ^{31}P NMR spectra were acquired between 295 K and 320 K on a 400 MHz spectrometer. Samples were prepared with 100 mg/mL DMPC and (a) 0 (0 %), (b) 40 (28.6 %), (c) 80 (44.4 %), or (d) 200 (66.7 %) mg/mL CQS in tris buffer (10 mM tris, 100 mM NaCl, pH 7.4).

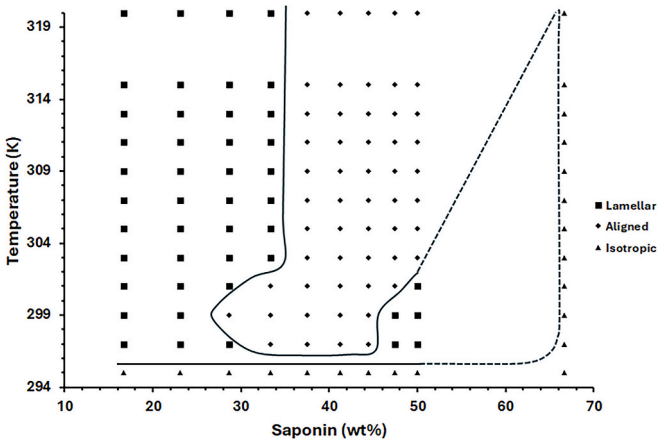

Fig. 3. Temperature-composition diagram of DMPC-CQS binary mixtures. The dominant phase was identified from ^{31}P NMR data as non-orienting lamellar (square), aligned in the magnetic field (diamond), or isotropic (triangle). Solid lines represent experimentally determined phase boundaries; dashed lines are hypothetical. All sample conditions with greater than 0 % CQS had an isotropic population, but it was not the dominant phase below 50 % CQS, except at 295 K. The full set of ^{31}P NMR spectra used to construct this diagram are provided in the Supporting Information as Fig. S3.

at approximately the same CQS mass fraction. Decreasing the ionic strength also strengthened alignment of particles formed with high CQS content, consistent with the effect of ionic strength on bicelle formation by DHPC and DMPC [82]; clear alignment was not observed in the ^{31}P NMR data for the 33.3 % CQS sample regardless of the ionic strength (Fig. 4b,c), but the 50 % CQS sample showed greater intensity in its aligned peak with 0 mM NaCl (Fig. 4d) than with 100 mM NaCl (Fig. 4e). Perhaps more strikingly, the isotropic peak was reduced in intensity at low ionic strength for both CQS fractions (Fig. 4b,d). The reduced isotropic population is consistent with our previous results, but we expected decreasing the ionic strength to also weaken alignment at high CQS content, and we observed the opposite. Thus, differences in ionic strength are not sufficient to explain the lack of consistency between our two sets of data. Instead, it is likely that batch-to-batch variations in the saponin composition and non-saponin impurities, such as sapogenins and carbohydrates, of the crude saponin extract are responsible.

3.3. Solubilization of DMPC by pure saponins

Coexistence of aligned and unoriented phases and poor reproducibility in the preparation of orienting bicelles present an obvious challenge to utilizing CQS-based bicelles in biomedical and research applications. We hypothesized that using purified saponins, both single molecules and natural saponin extracts devoid of non-saponin impurities, would allow the formation of a more homogeneous and reproducible aligned bicelle phase. Consequently, we selected seven additional saponin molecules or mixtures – pure *Quillaja* saponins (PQS), aescin, ginsenoside Rb1 (Grb1), digitonin, glycyrrhizic acid (GA), hederacoside C (HC), and α-hederin (αH) (structures in Fig. 5b) – and assayed them for solubilization of DMPC (Fig. 5a). PQS and aescin comprised plant-derived mixtures of saponin molecules but were purified of non-saponin impurities. All the saponins except αH solubilized DMPC below 80 % saponin content. αH is also not water-soluble and visibly did not dissolve in the aqueous mixtures with DMPC. Previous work reported αH interactions with lipid bilayers were mediated via sterols, so the absence of cholesterol in our samples may also have disfavored an interaction with the lipids [83,84]. The transmittance in samples with GA plateaued above 33 % GA content, which almost exactly matches the amount previously reported to produce an optically transparent solution (34 %) [50]. Most of the saponins caused a stable

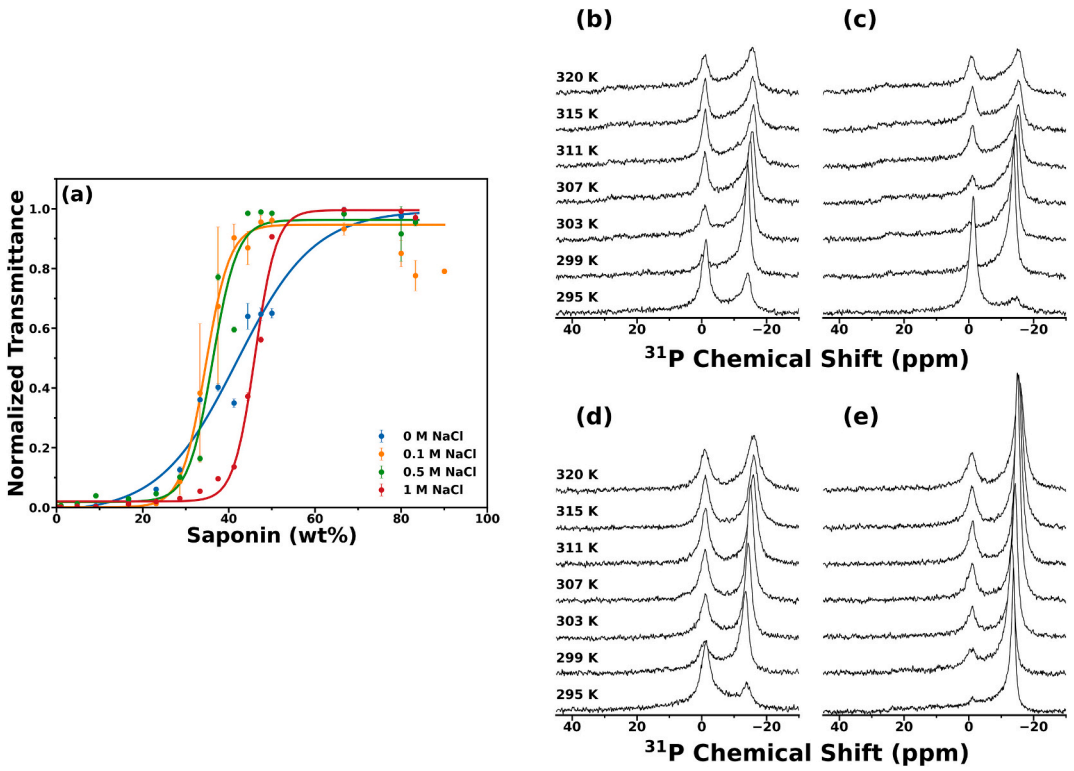

Fig. 4. Effect of ionic strength on solubilization of DMPC by CQS. (a) Transmittance assays for mixtures of DMPC and CQS with NaCl concentrations of 0 M (blue), 0.1 M (orange), 0.5 M (green), or 1 M (red). ^{31}P NMR spectra at the noted temperatures of 100 mg/mL DMPC with (b,c) 50 mg/mL CQS or (d,e) 100 mg/mL CQS and (b,d) 0 M NaCl or (c,e) 0.1 M NaCl. All transmittance data were fitted with Boltzmann sigmoids. The full fit parameters are provided in Table S1. Transmittance data plotted as a function of the mass ratio between the lipid and the saponin are provided in Fig. S1. (For interpretation of the references to colour in this figure legend, the reader is referred to the web version of this article.)

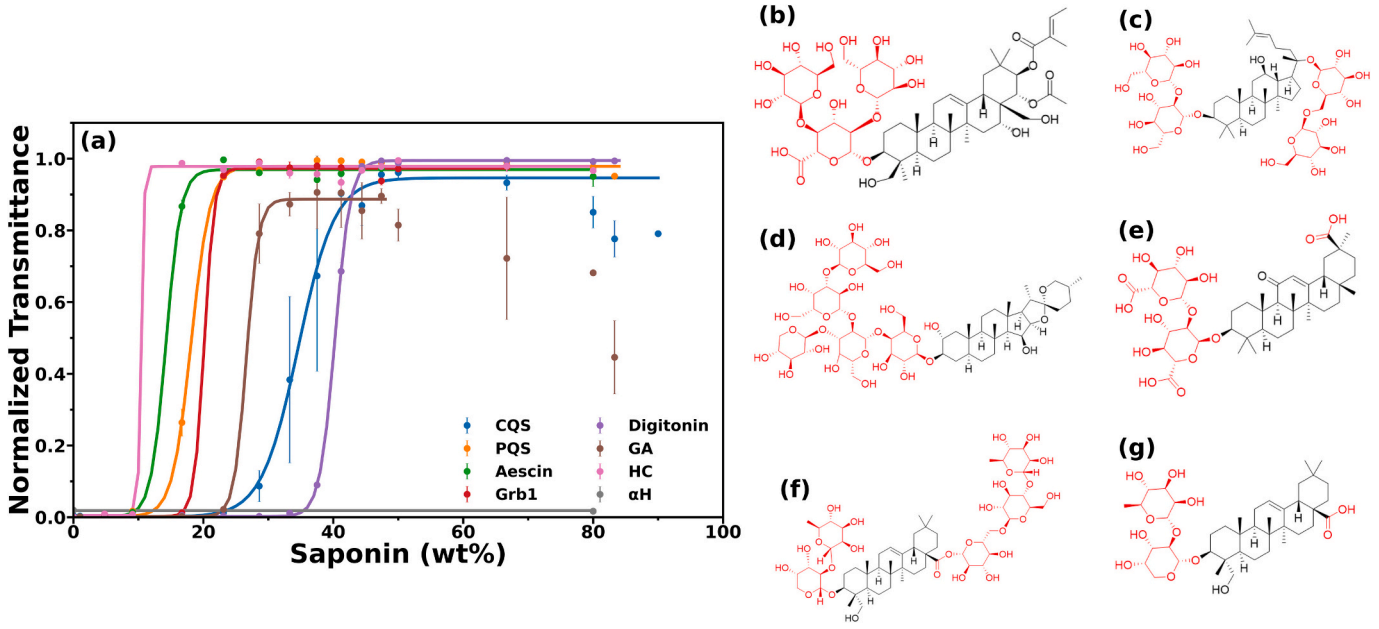

Fig. 5. Solubilization of DMPC by various saponins. (a) Transmittance was calculated from absorbance at 790 nm for mixtures of DMPC with CQS (blue), PQS (orange), aescin (green), Grb1 (red), digitonin (purple), GA (brown), HC (pink), or αH (grey) equilibrated at 298 K. DMPC concentration was held constant at 10 mg/mL in each sample and the saponin mass fraction is given relative to total surfactant concentration. Data were fitted to Boltzmann sigmoids. (b) Molecular structures of saponins are represented with the hydrophobic portion in black and the hydrophilic portions in red. The structure of β-aescin is shown as representative of the saponin structures in the aescin mixture. All transmittance data were fitted with Boltzmann sigmoids. The full fit parameters are provided in Table S1. Transmittance data plotted as a function of the mass ratio between the lipid and the saponin are provided in Fig. S1. (For interpretation of the references to colour in this figure legend, the reader is referred to the web version of this article.)

plateau in the transmittance, but samples with GA decreased transmittance in above 50 % GA (Fig. 5a, light green). These samples also became notably viscous or gel-like, which may have caused the sample to scatter light. Boltzmann sigmoids were fitted to the transmittance data for samples with the other saponins to quantitatively estimate the saponin mass fraction required to reach 50 % maximum transmittance (S_{50}). Digitonin required the greatest mass fraction to solubilize the phospholipid, with S_{50} of 40.3 %, and HC required the least, with S_{50} of 10.4 %.

S_{50} did not correlate obviously with any property of the saponins, including critical micelle concentration (CMC), solubility in water, molecular weight, or number of monosaccharide units. HC has the lowest reported CMC and the lowest measured S_{50}. But GA, which does not form micelles under these sample conditions, solubilized lipids more efficiently than digitonin, which does form micelles [16]. αH has little to no solubility in water and did not dissolve DMPC, while HC, which has the lowest water solubility of the remaining saponins, was the most efficient lipid solubilizer. Similarly, the two most water-soluble saponins, CQS and aescin, displayed very different lipid solubilization efficiencies, ranking second and sixth respectively among the saponins we tested. Previous research suggests that saponin interactions with lipid bilayers are highly structure-dependent [20]. Solubilization of hydrophobic drugs by saponin micelles was also shown to depend on saponin structure, with improved solubilization observed for bidesmosidic oleanane saponins compared to mono- and tri-desmosidic oleanane and steroid saponins [85]. The sample size of saponins here is not high enough to draw a concrete structure-activity relationship, but saponin structural features that may contribute positively to lipid solubilization based on our data are a triterpenoid backbone, hydrophilic substituents on opposite ends of the aglycone, and a double bond. More efficient solubilization by triterpenoid than by steroid saponins is consistent with the structural relationship described for solubilization of hydrophobic drugs by saponins [85]. Additionally, αH and HC are identical in their sapogenin domains and displayed significantly different lipid solubilization behaviors, so the carbohydrate chain structure must also play a role.

3.4. DMPC nanoparticles with GA, HC, and Grb1 form pure aligned phases

To determine whether the additional saponins could induce formation of bicelles that align in a magnetic field, we collected static ^{31}P NMR spectra of DMPC mixed with the saponins that solubilized DMPC (Fig. 6, **S4-S8**). The sample conditions giving the most homogeneous aligned phases with each saponin are presented in Fig. 6. At low temperature, an aescin-DMPC mixture with 20 % aescin produced a powder pattern with the perpendicular edge near −12.5 ppm. Above 303 K, the parallel edge of the powder pattern reduced to noise level, and the peak at the perpendicular edge became more symmetric, indicating the formation of planar lipid bilayers that aligned in the magnetic field. A skew toward higher frequency persisted in this temperature range, possibly representing a minor population of non-orienting lamellar particles. Similar samples were previously reported by Hellweg et al. to form planar membranes above 10 % aescin by mass [46,47]. This roughly corresponds to the aescin content we measured to begin solubilization of the lipid (see Fig. 5) but is lower than the aescin content that induced alignment in the magnetic field. A few factors might explain the seeming discrepancy between these observations. Spherical vesicles may have coexisted with bicelles below 20 % aescin, thereby hindering alignment. Alternatively, different sample conditions may have caused differences in the phase boundaries. Our samples contained higher ionic strength than those in the previous studies, and ionic strength affects the formation of orienting lipid bilayers, as discussed above. Hellweg et al. also used pure β-aescin, while our samples contained a mixture of triterpenoid saponins collectively called aescin, of which β-aescin is the primary component.

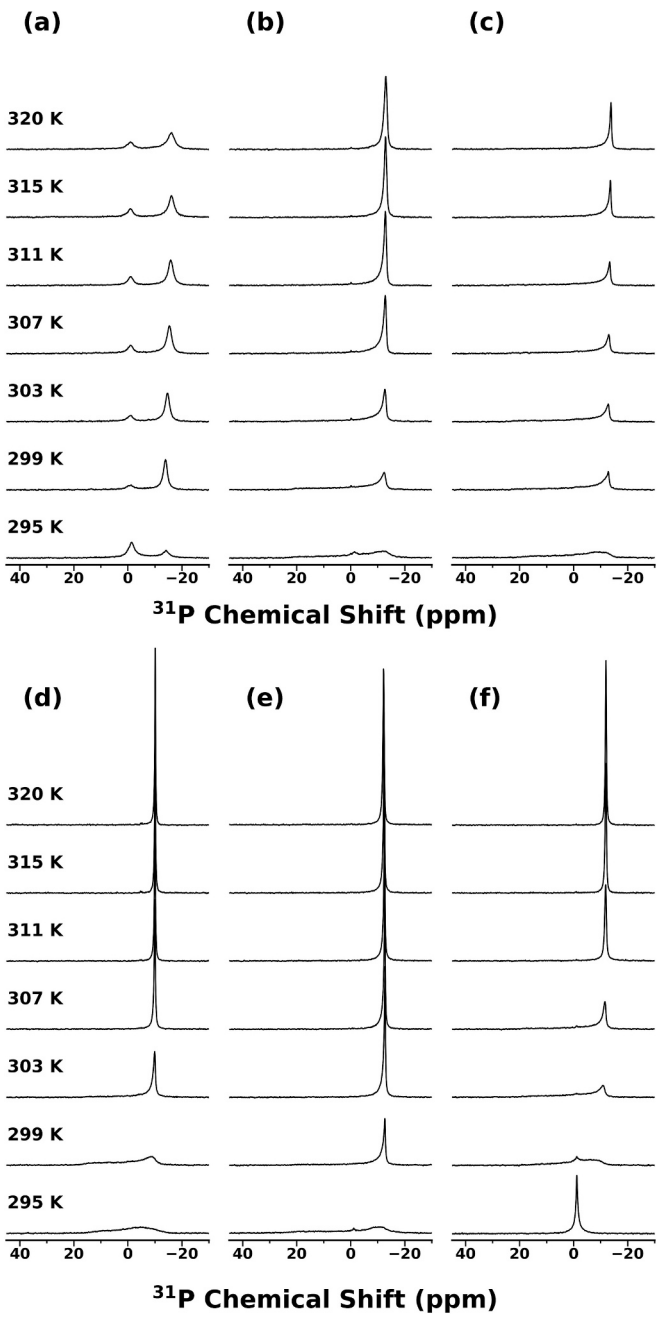

Fig. 6. Most homogeneous aligned phases for DMPC with different saponins. DMPC (100 mg/mL) was mixed with (a) 0.7× CQS, (b) 0.25× aescin, (c) 0.5× digitonin, (d) 0.2× GA, (e) 0.2× Grb1, and (f) 0.2× HC. ^{31}P NMR spectra were acquired from 295 K – 320 K on a 400 MHz spectrometer. Saponin structures are shown above the appropriate NMR spectra. Additional spectra of non-orienting samples prepared with each saponin are included in the Supporting Information as Figs. S4-S8.

DMPC mixtures with GA, Grb1, and HC produced single symmetric peaks near −12 ppm in the presence of Grb1 and HC or near −10 ppm in the presence of GA. These peaks appeared much narrower than the perpendicular edge of the DMPC powder pattern or the CQS-DMPC aligned peak, with widths less than 1/3 that of DMPC alone and 1/6 that of CQS-DMPC. The variation of the chemical shifts with temperature was also much smaller than for the CQS-DMPC samples. Taken together, these data indicate highly homogenous planar membranes that align in a magnetic field were formed by DMPC in the presence of GA, Grb1, and HC. GA and Grb1 samples transitioned from non-orienting

lamellar particles at 295 K to aligning particles at 303 K for Grb1 samples and 305 K for GA samples. Lipids with HC appeared isotropic at 295 K – 297 K, non-orienting lamellar from 299 K – 307 K, and aligned above 309 K. Alignment occurred at human body temperature with all three saponins. However, the range of compositions allowing bicelle alignment was narrow with each saponin (**Fig. S6-S8**); each system aligned with 16.7 % saponin, but alignment was not observed when the saponin content was decreased to 9.1 % or increased to 23.1 %. Based on the results with CQS-DMPC mixtures, we hypothesized that optimal bicelle alignment would be achieved with saponin content corresponding to the beginning of the plateau phase in the transmittance assay. In fact, DMPC with GA, HC, and Grb1 formed aligning bicelle phases with the exact same saponin mass fraction (16.7 %), despite having notably different S_{50} values measured in the transmittance assay. This may reflect a change in the temperature-composition behavior of DMPC-saponin mixtures at the higher temperatures and total surfactant concentrations used for NMR. But the samples with GA and Grb1, which did not appear transparent at this saponin content in the transmittance assay, also did not appear transparent during the NMR experiments. The sample with HC was clear in both experiments. This may also reflect different planar membrane structures. For example, GA and Grb1 might favor the formation of large light-scattering sheets, while HC might promote formation of smaller optically transparent sheets or nanodiscs. Previous work by Hellweg et al. showed that DMPC-GA particles became larger near the temperatures that we observed alignment, compared to the small bicelles they observed below the main phase transition temperature of DMPC (298 K) [50]. But they described these particles as vesicles and used higher GA content than in our samples. In any case, more research is needed to fully understand the nature of the particles that align during NMR experiments.

Like with aescin, lipids with 33 % digitonin exhibited a powder pattern at low temperature, and the parallel edge reduced in intensity as the temperature increased. However, the powder pattern lineshape never completely disappeared at this digitonin content or any others we tested (**Fig. S5**). The intensity of the perpendicular edge relative to the parallel edge was greater for the sample with digitonin than for DMPC alone, so there may be an aligned bicelle phase present, but the powder pattern population appeared to dominate the lineshape. Thus, DMPC does not appear to form homogeneous bicelles that align in the magnetic field in the presence of digitonin. Compared to the saponins that formed planar membranes with DMPC, digitonin has a larger aglycone ring structure, comprising six fused rings rather than four for Grb1 or five for the remaining saponins. It is also the only saponin tested here that has a steroid rather than a triterpenoid sapogenin. In the context of lipid solubilization, the size of the ring system in the sapogenin may be analogous to a detergent or phospholipid alkyl chain length, and so the longer chain length disfavors lipid solubilization and formation of bicelles.

4. Conclusion

In summary, we comprehensively characterized the lipid solubilization behavior of several saponins by optical spectroscopy and solid-state NMR. We constructed a temperature-composition diagram of the CQS-DMPC system to delineate the boundaries between non-orienting lamellar, planar aligning, and isotropic phases, though ^{31}P NMR lineshapes indicated significant heterogeneity. Formation of the planar aligned phase was favored by low ionic strength but demonstrated significant batch-to-batch variation. To improve sample homogeneity and reproducibility of bicelle alignment for use in anisotropy-based NMR experiments and reconstitution of membrane proteins, we explored the lipid solubilization behavior of pure saponins. The triterpenoid saponins aescin, GA, HC, and Grb1 efficiently solubilized DMPC and induced the formation of bicelles that aligned in a magnetic field, while the steroid saponin digitonin was a less efficient lipid solubilizer and did not allow formation of pure bicelles. GA, Grb1, and HC are particularly promising for producing planar membranes for biomedical and research applications. Compared to DHPC, the traditional bicelle belt molecule, saponins are much larger and chemically distinct from the phospholipids, and therefore may engage in molecular interactions, especially hydrogen bonding, that DHPC would not. However, the saponins offer several advantages. To our knowledge, GA is the least expensive bicelle belt molecule reported to date. GA and HC are also relatively nontoxic, and GA does not form micelles that could contaminate bicelle samples [16]. Grb1 and HC are more costly than GA but are nonionic and thus allow formation of membranes without worry of electrostatic interactions involving the belt. Saponins being chemically distinct from the phospholipids and considerably bulkier may also prevent some interactions that DHPC would not. For example, some smaller proteins or peptides might penetrate both the rim and bilayer portions of a DHPC bicelle because the DHPC molecules are chemically similar to the longer chain phospholipids, while the larger saponins would prevent that penetration of the rim. The specific advantages and disadvantages of each bicelle platform will likely need to be evaluated on a case-by-case basis.

Regardless, more research is needed to directly evaluate the ability of the saponin-lipid particles to enable anisotropy-based NMR experiments and to reconstitute membrane proteins. Further research should assess the toxicity of these particles to determine their suitability for biomedical applications. For producing membranes that mimic physiological conditions, the saponins should also be evaluated for their ability to accommodate anionic lipids in bicelles. Aescin, for example, was previously shown to not mix with DOPG, and GA was only found to form vesicles with DOPG [86,87]. The capacity to form membranes with anionic lipids may also indicate whether these saponins could be capable of direct extraction of membrane proteins and physiological lipids from biological membranes. In addition, as the ^{31}P NMR data does not directly report particle shape, the bicelles described here, which we broadly defined as any non-spherical mixed bilayer micelle, might adopt discoidal, cylindrical, rectangular, or other geometries, and these morphologies may depend on temperature and composition. Electron microscopy or x-ray scattering experiments would be useful to identify the morphologies of these particles. Lastly, it would be revealing to evaluate lipid solubilization by a larger sample of saponin structures. This would provide a fuller understanding of the structural determinants of lipid solubilization and bicelle formation and allow for the rational design of synthetic saponins for use in lipid nanoparticles for therapeutic and research purposes.

CRediT authorship contribution statement

Samuel D. McCalpin: Writing – review & editing, Writing – original draft, Visualization, Validation, Supervision, Methodology, Investigation, Formal analysis, Data curation, Conceptualization. **Kailey Kassinger:** Investigation, Formal analysis. **Madison Gilmore:** Investigation, Formal analysis. **Ayyalusamy Ramamoorthy:** Writing – review & editing, Supervision, Resources, Project administration, Methodology, Investigation, Funding acquisition, Conceptualization.

Declaration of competing interest

The authors declare that they have no known competing financial interests or personal relationships that could have appeared to influence the work reported in this paper.

Acknowledgements

Funding was provided by the National Institutes of Health grant R35GM13973. A portion of this work was performed at the National High Magnetic Field Laboratory, which is supported by National Science Foundation Cooperative Agreement No. DMR-2128556* and the State of Florida.

Appendix A. Supplementary data

Supplementary data to this article can be found online at https://doi.org/10.1016/j.jcis.2025.139008.

Data availability

All data files are freely available at the Open Science Framework.

References

[1] M. Kanlayavattanakul, D. Mersni, N. Lourith, Plant-derived Saponins and their prospective for cosmetic and personal care products, Bot. Stud. 65 (1) (2024) 32, https://doi.org/10.1186/s40529-024-00438-8.

[2] R. Kaur, V. Mishra, S. Gupta, S. Sharma, A. Vaishnav, S.V. Singh, Industrial and environmental applications of plant-derived Saponins: an overview and future prospective, J. Plant Growth Regul. 43 (9) (2024) 3012–3026, https://doi.org/10.1007/s00344-023-11201-x.

[3] K. Sharma, R. Kaur, S. Kumar, R.K. Saini, S. Sharma, S.V. Pawde, V. Kumar, Saponins: a concise review on food related aspects, applications and health implications, Food Chem. Adv. 2 (2023) 100191, https://doi.org/10.1016/j.focha.2023.100191.

[4] C.D. Adenutsi, J.N. Turkson, L. Wang, G. Zhao, T. Zhang, J.A. Quaye, S. Erzuah, Y. A. Sokama-Neuyam, Review on potential application of Saponin-based natural surfactants for green chemical enhanced oil recovery: perspectives and progresses, Energy Fuel 37 (13) (2023) 8781–8823, https://doi.org/10.1021/acs.energyfuels.3c00627.

[5] Y.P. Timilsena, A. Phosanam, R. Stockmann, Perspectives on Saponins: food functionality and applications, Int. J. Mol. Sci. 24 (17) (2023) 13538, https://doi.org/10.3390/ijms241713538.

[6] T.B. Schreiner, M.M. Dias, M.F. Barreiro, S.P. Pinho, Saponins as natural emulsifiers for Nanoemulsions, J. Agric. Food Chem. 70 (22) (2022) 6573–6590, https://doi.org/10.1021/acs.jafc.1c07893.

[7] S. Rai, E. Acharya-Siwakoti, A. Kafle, H.P. Devkota, A. Bhattarai, Plant-derived Saponins: a review of their surfactant properties and applications, Sci 3 (4) (2021) 44, https://doi.org/10.3390/sci3040044.

[8] Y. Liao, Z. Li, Q. Zhou, M. Sheng, Q. Qu, Y. Shi, J. Yang, L. Lv, X. Dai, X. Shi, Saponin surfactants used in drug delivery systems: a new application for natural medicine components, Int. J. Pharm. 603 (2021) 120709, https://doi.org/10.1016/j.ijpharm.2021.120709.

[9] P. Wang, Natural and synthetic Saponins as vaccine adjuvants, Vaccines 9 (3) (2021) 222, https://doi.org/10.3390/vaccines9030222.

[10] M.M. El Aziz, A. Ashour, A.S. Melad, A review on Saponins from medicinal plants: chemistry, isolation, and determination, J. Nanomedicine Res. (2019), https://doi.org/10.15406/jnmr.2019.07.00199. Volume 7 (Issue 4).

[11] D. Oakenfull, G.S. Sidhu, Saponins, CRC Press, In Toxicants of Plant Origin, 1989.

[12] D. Oakenfull, Saponins in food—a review, Food Chem. 7 (1) (1981) 19–40, https://doi.org/10.1016/0308-8146(81)90019-4.

[13] J.M. Augustin, V. Kuzina, S.B. Andersen, S. Bak, Molecular activities, biosynthesis and evolution of triterpenoid Saponins, Phytochemistry 72 (6) (2011) 435–457, https://doi.org/10.1016/j.phytochem.2011.01.015.

[14] J.-P. Vincken, L. Heng, A. de Groot, H. Gruppen, Saponins, classification and occurrence in the plant kingdom, Phytochemistry 68 (3) (2007) 275–297, https://doi.org/10.1016/j.phytochem.2006.10.008.

[15] B. Korchowiec, M. Gorczyca, K. Wojszko, M. Janikowska, M. Henry, E. Rogalska, Impact of Two Different Saponins on the Organization of Model Lipid Membranes, Biochim. Biophys. Acta BBA - Biomembr. (**2015**), https://doi.org/10.1016/j.bbamem.2015.06.007. *1848* (10, Part A), 1963–1973.

[16] S. Böttger, K. Hofmann, M.F. Melzig, Saponins can perturb biologic membranes and reduce the surface tension of aqueous solutions: a correlation? Bioorg. Med. Chem. 20 (9) (2012) 2822–2828, https://doi.org/10.1016/j.bmc.2012.03.032.

[17] E. Baumann, G. Stoya, A. Völkner, W. Richter, C. Lemke, W. Linss, Hemolysis of human erythrocytes with Saponin affects the membrane structure, Acta Histochem. 102 (1) (2000) 21–35, https://doi.org/10.1078/0065-1281-00534.

[18] P.H. Demana, N.M. Davies, S. Hook, T. Rades, Analysis of Quil A–Phospholipid Mixtures Using Drift Spectroscopy, Int. J. Pharm. 342 (1) (2007) 49–61, https://doi.org/10.1016/j.ijpharm.2007.04.030.

[19] C. Gauthier, J. Legault, K. Girard-Lalancette, V. Mshvildadze, A. Pichette, Haemolytic activity, cytotoxicity and membrane cell Permeabilization of semi-synthetic and natural Lupane- and Oleanane-type Saponins, Bioorg. Med. Chem. 17 (5) (2009) 2002–2008, https://doi.org/10.1016/j.bmc.2009.01.022.

[20] H. Lorent, J. Quetin-Leclercq, M.-P. Mingeot-Leclercq, The amphiphilic nature of Saponins and their effects on artificial and biological membranes and potential consequences for red blood and Cancer cells, Org. Biomol. Chem. 12 (44) (2014) 8803–8822, https://doi.org/10.1039/C4OB01652A.

[21] K. Wojciechowski, M. Orczyk, T. Gutberlet, T. Geue, Complexation of phospholipids and cholesterol by Triterpenic Saponins in bulk and in monolayers, Biochim. Biophys. Acta BBA - Biomembr. 1858 (2) (2016) 363–373, https://doi.org/10.1016/j.bbamem.2015.12.001.

[22] C. Groot, de; Müller-Goymann, C. C., Saponin interactions with model membrane systems – Langmuir monolayer studies, hemolysis and formation of ISCOMs, Planta Med. 82 (2016) 1496–1512, https://doi.org/10.1055/s-0042-118387.

[23] M. Chen, V. Balhara, A.M. Jaimes Castillo, J. Balsevich, L.J. Johnston, Interaction of Saponin 1688 with phase separated lipid bilayers, Biochim. Biophys. Acta BBA - Biomembr. 1859 (7) (2017) 1263–1272, https://doi.org/10.1016/j.bbamem.2017.03.024.

[24] B. Morein, K. Lövgren, B. Rönnberg, A. Sjölander, M. Villacrés-Eriksson, Immunostimulating Complexes, Clin. Immunother. 3 (6) (1995) 461–475, https://doi.org/10.1007/BF03259065.

[25] J.B. Press, R.C. Reynolds, R.D. May, D.J. Marciani, Structure/Function Relationships of Immunostimulating Saponins. In *Studies in Natural Products Chemistry*; Atta-ur-Rahman, Ed.; Bioactive Natural Products (Part E), Elsevier 24 (2000) 131–174, https://doi.org/10.1016/S1572-5995(00)80045-9.

[26] A.V. Rao, D.M. Gurfinkel, The bioactivity of Saponins: triterpenoid and steroidal glycosides, Drug Metabol. Drug Interact. 17 (1–4) (2000) 211–236, https://doi.org/10.1515/DMDI.2000.17.1-4.211.

[27] X. Cui, X. Ma, C. Li, H. Meng, C. Han, A Review: Structure–Activity Relationship between Saponins and Cellular Immunity, Mol. Biol. Rep. 50 (3) (2023) 2779–2793, https://doi.org/10.1007/s11033-022-08233-z.

[28] D.J. Marciani, Elucidating the mechanisms of action of Saponin-derived adjuvants, Trends Pharmacol. Sci. 39 (6) (2018) 573–585, https://doi.org/10.1016/j.tips.2018.03.005.

[29] P.P. Brindha, Role of phytochemicals as immunomodulatory agents: a review, Int. J. Green Pharm. IJGP 10 (1) (2016), https://doi.org/10.22377/ijgp.v10i1.600.

[30] D.J. Marciani, Is Fucose the answer to the immunomodulatory paradox of Quillaja Saponins? Int. Immunopharmacol. 29 (2) (2015) 908–913, https://doi.org/10.1016/j.intimp.2015.10.028.

[31] B.N. Smith, R.N. Dilger, Immunomodulatory potential of dietary soybean-derived Isoflavones and Saponins in Pigs1, J. Anim. Sci. 96 (4) (2018) 1288–1304, https://doi.org/10.1093/jas/sky036.

[32] L. Shen, H. Luo, L. Fan, X. Tian, A. Tang, X. Wu, K. Dong, Z. Su, Potential Immunoregulatory mechanism of plant Saponins: a review, Molecules 29 (1) (2024) 113, https://doi.org/10.3390/molecules29010113.

[33] F.R.S. Passos, H.G. Araújo-Filho, B.S. Monteiro, S. Shanmugam, A.A.S. de Araújo, J. R.G.S. da Almeida, P. Thangaraj, L.J.Q. Júnior, J.S.S. de Quintans, Anti-inflammatory and modulatory effects of steroidal Saponins and Sapogenins on cytokines: a review of pre-clinical research, Phytomedicine 96 (2022) 153842, https://doi.org/10.1016/j.phymed.2021.153842.

[34] J. Dong, W. Liang, T. Wang, J. Sui, J. Wang, Z. Deng, D. Chen, Saponins regulate intestinal inflammation in Colon Cancer and IBD, Pharmacol. Res. 144 (2019) 66–72, https://doi.org/10.1016/j.phrs.2019.04.010.

[35] J.M.R. Patlolla, C.V. Rao, Anti-inflammatory and anti-Cancer properties of β-Escin, a triterpene Saponin, Curr. Pharmacol. Rep. 1 (3) (2015) 170–178, https://doi.org/10.1007/s40495-015-0019-9.

[36] T. Wijesekara, J. Luo, B. Xu, Critical review on anti-inflammation effects of Saponins and their molecular mechanisms, Phytother. Res. 38 (4) (2024) 2007–2022, https://doi.org/10.1002/ptr.8164.

[37] C.R. Kensil, R. Kammer, QS-21: a water-soluble triterpene glycoside adjuvant, Expert Opin. Investig. Drugs 7 (9) (1998) 1475–1482, https://doi.org/10.1517/13543784.7.9.1475.

[38] Z.I. Rajput, S. Hu, C. Xiao, A.G. Arijo, Adjuvant effects of Saponins on animal immune responses, J. Zhejiang Univ. Sci. B 8 (3) (2007) 153–161, https://doi.org/10.1631/jzus.2007.B0153.

[39] J.M. Reimer, K.H. Karlsson, K. Lövgren-Bengtsson, S.E. Magnusson, A. Fuentes, L. Stertman, Matrix-M™ adjuvant induces local recruitment, activation and maturation of central immune cells in absence of antigen, PloS One 7 (7) (2012) e41451, https://doi.org/10.1371/journal.pone.0041451.

[40] G. Singh, S. Song, E. Choi, P.-B. Lee, F.S. Nahm, Recombinant zoster vaccine (Shingrix®): a new option for the prevention of herpes zoster and Postherpetic neuralgia, Korean J. Pain 33 (3) (2020) 201–207, https://doi.org/10.3344/kjp.2020.33.3.201.

[41] A. Ghaemi, P. Roshani Asl, H. Zargaran, D. Ahmadi, A.A. Hashimi, E. Abdolalipour, S. Bathaeian, S.M. Miri, Recombinant COVID-19 vaccine based on recombinant RBD/nucleoprotein and Saponin adjuvant induces long-lasting neutralizing antibodies and cellular immunity, Front. Immunol. (2022) 13, https://doi.org/10.3389/fimmu.2022.974364.

[42] I. Podolak, A. Galanty, D. Sobolewska, Saponins as cytotoxic agents: a review, Phytochem. Rev. 9 (3) (2010) 425–474, https://doi.org/10.1007/s11101-010-9183-z.

[43] Z. Chen, H. Duan, X. Tong, P. Hsu, L. Han, S.L. Morris-Natschke, S. Yang, W. Liu, K.-H. Lee, Cytotoxicity, hemolytic toxicity, and mechanism of action of Pulsatilla Saponin D and its synthetic derivatives, J. Nat. Prod. 81 (3) (2018) 465–474, https://doi.org/10.1021/acs.jnatprod.7b00578.

[44] Y. Wang, Y. Zhang, Z. Zhu, S. Zhu, Y. Li, M. Li, B. Yu, Exploration of the correlation between the structure, hemolytic activity, and cytotoxicity of steroid Saponins, Bioorg. Med. Chem. 15 (7) (2007) 2528–2532, https://doi.org/10.1016/j.bmc.2007.01.058.

[45] L. Voutquenne, Lavaud Catherine, Massiot Georges, L.L. Men-Olivier, Structure-activity relationships of Haemolytic Saponins, Pharm. Biol. 40 (4) (2002) 253–262, https://doi.org/10.1076/phbi.40.4.253.8470.

[46] R. Geisler, M.C. Pedersen, Y. Hannappel, R. Schweins, S. Prévost, R. Dattani, L. Arleth, T. Hellweg, Aescin-induced conversion of gel-phase lipid membranes into Bicelle-like lipid nanoparticles, Langmuir 35 (49) (2019) 16244–16255, https://doi.org/10.1021/acs.langmuir.9b02077.

[47] R. Sreij, C. Dargel, Y. Hannappel, J. Jestin, S. Prévost, R. Dattani, O. Wrede, T. Hellweg, Temperature dependent self-organization of DMPC membranes promoted by intermediate amounts of the Saponin Aescin, Biochim. Biophys. Acta

BBA - Biomembr. 1861 (5) (2019) 897–906, https://doi.org/10.1016/j.bbamem.2019.01.015.
[48] R. Geisler, S. Prévost, R. Dattani, T. Hellweg, Effect of cholesterol and ibuprofen on DMPC-β-Aescin Bicelles: a temperature-dependent wide-angle X-ray scattering study, Crystals 10 (5) (2020) 401, https://doi.org/10.3390/cryst10050401.
[49] R. Geisler, C. Dargel, T. Hellweg, The biosurfactant β-Aescin: a review on the Physico-chemical properties and its interaction with lipid model membranes and Langmuir monolayers, Molecules 25 (1) (2020) 117, https://doi.org/10.3390/molecules25010117.
[50] C. Dargel, Y. Hannappel, T. Hellweg, Heating-induced DMPC/glycyrrhizin Bicelle-to-vesicle transition: a X-ray contrast variation study, Biophys. J. 118 (10) (2020) 2411–2425, https://doi.org/10.1016/j.bpj.2020.03.022.
[51] R. Geisler, M. Cramer Pedersen, N. Preisig, Y. Hannappel, S. Prévost, R. Dattani, L. Arleth, T. Hellweg, Aescin – a natural soap for the formation of lipid Nanodiscs with tunable size, Soft Matter 17 (7) (2021) 1888–1900, https://doi.org/10.1039/D0SM02043E.
[52] F. Escobedo, M. Gospalswamy, P. Hägerbäumer, T.J. Stank, J. Victor, G. Groth, H. Gohlke, C. Dargel, T. Hellweg, M. Etzkorn, Characterization of size-Tuneable Aescin-lipid nanoparticles as platform for stabilization of membrane proteins, Colloids Surf. B Biointerfaces 242 (2024) 114071, https://doi.org/10.1016/j.colsurfb.2024.114071.
[53] C. Dargel, L.H. Moleiro, A. Radulescu, T.J. Stank, T. Hellweg, Decomposition of mixed DMPC-Aescin vesicles to Bicelles is linked to the lipid's Main phase transition: a direct evidence by using chain-deuterated lipid, J. Colloid Interface Sci. (2024), https://doi.org/10.1016/j.jcis.2024.10.074.
[54] S.D. McCalpin, T. Ravula, A. Ramamoorthy, Saponins form nonionic lipid Nanodiscs for protein structural studies by nuclear magnetic resonance spectroscopy, J. Phys. Chem. Lett. (2022) 1705–1712, https://doi.org/10.1021/acs.jpclett.1c04185.
[55] M.-P. Nieh, V.A. Raghunathan, C.J. Glinka, T.A. Harroun, G. Pabst, J. Katsaras, Magnetically Alignable phase of phospholipid "Bicelle" mixtures is a chiral Nematic made up of wormlike micelles, Langmuir 20 (19) (2004) 7893–7897, https://doi.org/10.1021/la048641l.
[56] W.C. Leite, Y. Wu, S.V. Pingali, R.L. Lieberman, V.S. Urban, Change in morphology of Dimyristoylphosphatidylcholine/bile salt derivative Bicelle assemblies with Dodecylmaltoside in the disk and ribbon phases, J. Phys. Chem. Lett. 13 (42) (2022) 9834–9840, https://doi.org/10.1021/acs.jpclett.2c02445.
[57] M.-P. Nieh, C.J. Glinka, S. Krueger, R.S. Prosser, J. Katsaras, SANS study of the structural phases of magnetically Alignable lanthanide-doped phospholipid mixtures, Langmuir 17 (9) (2001) 2629–2638, https://doi.org/10.1021/la001567w.
[58] T.A. Harroun, M. Koslowsky, M.-P. Nieh, C.-F. de Lannoy, V.A. Raghunathan, J. Katsaras, Comprehensive examination of Mesophases formed by DMPC and DHPC mixtures, Langmuir 21 (12) (2005) 5356–5361, https://doi.org/10.1021/la050018t.
[59] E.J. Dufourc, Bicelles and Nanodiscs for biophysical chemistry11A tribute to prof Michèle auger, university Laval, Canada, Biochim. Biophys. Acta BBA - Biomembr. 1863 (1) (2021) 183478, https://doi.org/10.1016/j.bbamem.2020.183478.
[60] J. Amengual, L. Notaro-Roberts, M.-P. Nieh, Morphological control and modern applications of Bicelles, Biophys. Chem. 302 (2023) 107094, https://doi.org/10.1016/j.bpc.2023.107094.
[61] C.R. Sanders, B.J. Hare, K.P. Howard, J.H. Prestegard, Magnetically-oriented phospholipid micelles as a tool for the study of membrane-associated molecules, Prog. Nucl. Magn. Reson. Spectrosc. 26 (1994) 421–444, https://doi.org/10.1016/0079-6565(94)80012-X.
[62] U.H.N. Dürr, M. Gildenberg, A. Ramamoorthy, The magic of Bicelles lights up membrane protein structure, Chem. Rev. 112 (11) (2012) 6054–6074, https://doi.org/10.1021/cr300061w.
[63] T. Murakami, Phospholipid Nanodisc engineering for drug delivery systems, Biotechnol. J. 7 (6) (2012) 762–767, https://doi.org/10.1002/biot.201100508.
[64] J. Bariwal, H. Ma, A. Altenberg, H. Liang, Nanodiscs: a versatile Nanocarrier platform for Cancer diagnosis and treatment, Chem. Soc. Rev. 51 (5) (2022) 1702–1728, https://doi.org/10.1039/D1CS01074C.
[65] R. Kuai, L.J. Ochyl, K.S. Bahjat, A. Schwendeman, J.J. Moon, Designer vaccine Nanodiscs for personalized Cancer immunotherapy, Nat. Mater. 16 (4) (2017) 489–496, https://doi.org/10.1038/nmat4822.
[66] I. Noh, Z. Guo, R. Wang, A.T. Zhu, N. Krishnan, A. Mohapatra, W. Gao, R.H. Fang, L. Zhang, Modular functionalization of cellular Nanodiscs enables targeted delivery of chemotherapeutics into tumors, J. Control. Release 378 (2025) 145–152, https://doi.org/10.1016/j.jconrel.2024.12.004.
[67] C.R. Garcia, T. Rad Armin, Saeedinejad Farnoosh, Manojkumar Arvind, Roy Deepa, Rodrigo Hansapani, Chew Sue Anne, Rahman Ziyaur, Nieh Mu-Ping, U. Roy, Effect of drug-to-lipid ratio on Nanodisc-based Tenofovir drug delivery to the brain for HIV-1 infection, Nanomed 17 (13) (2022) 959–978, https://doi.org/10.2217/nnm-2022-0043.
[68] E.L. Dane, A. Belessiotis-Richards, C. Backlund, J. Wang, K. Hidaka, L.E. Milling, S. Bhagchandani, M.B. Melo, S. Wu, N. Li, N. Donahue, K. Ni, L. Ma, M. Okaniwa, M.M. Stevens, A. Alexander-Katz, D.J. Irvine, STING agonist delivery by tumour-penetrating PEG-lipid Nanodiscs primes robust anticancer immunity, Nat. Mater. 21 (6) (2022) 710–720, https://doi.org/10.1038/s41563-022-01251-z.
[69] T. Ravula, N.Z. Hardin, A. Ramamoorthy, Polymer Nanodiscs: advantages and limitations, Chem. Phys. Lipids 219 (2019) 45–49, https://doi.org/10.1016/j.chemphyslip.2019.01.010.
[70] M. Esmaili, M.A. Eldeeb, A.A. Moosavi-Movahedi, Current developments in native Nanometric discoidal membrane bilayer formed by amphipathic polymers, Nanomaterials 11 (7) (2021) 1771, https://doi.org/10.3390/nano11071771.
[71] J.M. Pettersen, Y. Yang, A.S. Robinson, Advances in Nanodisc platforms for membrane protein purification, Trends Biotechnol. 41 (8) (2023) 1041–1054, https://doi.org/10.1016/j.tibtech.2023.02.006.
[72] M.T. Odenkirk, G. Zhang, M.T. Marty, Do Nanodisc assembly conditions affect natural lipid uptake? J. Am. Soc. Mass Spectrom. 34 (9) (2023) 2006–2015, https://doi.org/10.1021/jasms.3c00170.
[73] H. Wu, K. Su, X. Guan, M.E. Sublette, R.E. Stark, Assessing the size, stability, and utility of Isotropically tumbling Bicelle Systems for Structural Biology, Biochim. Biophys. Acta BBA - Biomembr. 1798 (3) (2010) 482–488, https://doi.org/10.1016/j.bbamem.2009.11.004.
[74] M. Hoffmann, J. Eisermann, F.A. Schöffmann, M. Das, C. Vargas, S. Keller, D. Hinderberger, Influence of different polymer belts on lipid properties in Nanodiscs characterized by CW EPR spectroscopy, Biochim. Biophys. Acta BBA - Biomembr. 1863 (10) (2021) 183681, https://doi.org/10.1016/j.bbamem.2021.183681.
[75] A. Viegas, T. Viennet, M. Etzkorn, The power, pitfalls and potential of the Nanodisc system for NMR-based studies, Biol. Chem. 397 (12) (2016) 1335–1354, https://doi.org/10.1515/hsz-2016-0224.
[76] T. Ravula, Z. Hardin, J. Bai, S.-C. Im, L. Waskell, A. Ramamoorthy, Effect of polymer charge on functional reconstitution of membrane proteins in polymer Nanodiscs, Chem. Commun. 54 (69) (2018) 9615–9618, https://doi.org/10.1039/C8CC04184A.
[77] M.N. Triba, D.E. Warschawski, P.F. Devaux, Reinvestigation by phosphorus NMR of lipid distribution in Bicelles, Biophys. J. 88 (3) (2005) 1887–1901, https://doi.org/10.1529/biophysj.104.055061.
[78] K. Arnold, S. Ohki, M. Krumbiegel, Interaction of dextran sulfate with phospholipid surfaces and liposome aggregation and fusion, Chem. Phys. Lipids 55 (3) (1990) 301–307, https://doi.org/10.1016/0009-3084(90)90168-q.
[79] D. Huster, K. Arnold, Ca2+−mediated interaction between dextran sulfate and Dimyristoyl-Sn-Glycero-3-Phosphocholine surfaces studied by 2H nuclear magnetic resonance, Biophys. J. 75 (2) (1998) 909–916, https://doi.org/10.1016/S0006-3495(98)77579-4.
[80] A. Kezwon, K. Wojciechowski, Interaction of *Quillaja* bark Saponins with food-relevant proteins, Adv. Colloid Interface Sci. 209 (2014) 185–195, https://doi.org/10.1016/j.cis.2014.04.005.
[81] T. Hellweg, T. Sottmann, J. Oberdisse, Recent advances in biosurfactant-based association colloids—self-assembly in water, Front. Soft Matter (2023) 2, https://doi.org/10.3389/frsfm.2022.1081877.
[82] G. Raffard, S. Steinbruckner, A. Arnold, J.H. Davis, E.J. Dufourc, Temperature−composition diagram of Dimyristoylphosphatidylcholine−Dicaproylphosphatidylcholine "Bicelles" self-orienting in the magnetic field. A solid state 2H and 31P NMR study, Langmuir 16 (20) (2000) 7655–7662, https://doi.org/10.1021/la000564g.
[83] J. Lorent, C.S.L. Duff, J. Quetin-Leclercq, M.-P. Mingeot-Leclercq, Induction of highly curved structures in relation to membrane Permeabilization and budding by the triterpenoid Saponins, α- and δ-Hederin, J. Biol. Chem. 288 (20) (2013) 14000–14017, https://doi.org/10.1074/jbc.M112.407635.
[84] J. Lorent, L. Lins, Ò. Domenech, J. Quetin-Leclercq, R. Brasseur, M.-P. Mingeot-Leclercq, Domain formation and Permeabilization induced by the Saponin α-Hederin and its Aglycone Hederagenin in a cholesterol-containing bilayer, Langmuir 30 (16) (2014) 4556–4569, https://doi.org/10.1021/la4049902.
[85] Z. Vinarov, D. Radeva, V. Katev, S. Tcholakova, N. Denkov, Solubilisation of hydrophobic drugs by Saponins, Indian J. Pharm. Sci. 80 (4) (2018), https://doi.org/10.4172/pharmaceutical-sciences.1000411.
[86] F. Gräbitz-Bräuer, C. Dargel, R. Geisler, P. Fandrich, V. Sabadasch, L. Porcar, A. Mix, T. Hellweg, Coexistence of DOPG Model Membranes and β-Aescin Micelles: A Combined Scattering and NMR Study, Colloid Polym. Sci. 301 (12) (2023) 1499–1512, https://doi.org/10.1007/s00396-023-05168-0.
[87] C. Dargel, F. Gräbitz-Bräuer, R. Geisler, P. Fandrich, Y. Hannappel, L. Porcar, T. Hellweg, Stable DOPG/glycyrrhizin vesicles with a wide range of mixing ratios: structure and stability as seen by scattering experiments and Cryo-TEM, Molecules 26 (16) (2021) 4959, https://doi.org/10.3390/molecules26164959.